ONLINE FIRST January 28, 2025

Engineering Transactions, **73**, https://doi.org/10.24423/engtrans.3428.2025
Institute of Fundamental Technological Research Polish Academy of Sciences (IPPT PAN)
Université de Lorraine • Poznan University of Technology

OSA 2024

Modeling of the Acoustic Properties of Foamed Polypropylene Panels

Patrycja Świrk, Lucyna Leniowska

Department of Mechatronics and Control Engineering, University of Rzeszów
Rzeszów, Poland

*Corresponding Author e-mail: pswirk@ur.edu.pl

This article presents research on modelling baffles with the desired properties of the sound absorption coefficient (SAC). The purpose of the study was to model and compare the SAC values based on selected theoretical models with the results obtained from measurements of this coefficient in panels made of foamed polypropylene. The assessment of sound absorption properties was carried out using two theoretical models: the Johnson–Champoux–Allard (JCA) model and the Sgard model. The accuracy of the calculated SAC was verified based on laboratory measurements of this parameter for selected material configurations, using the technique of two microphones in an impedance tube. Both theoretical and experimental studies were conducted on porous materials in the form of granules. The application of the Sgard model yielded the best results, with the smallest discrepancies in relation to the experimental tests. The results can be used to improve the SAC and efficiency of acoustic panels whose basic material is foamed polypropylene.

Keywords: perforated porous material; sound absorption coefficient; double porosity.

1. Introduction

Porous structures have been widely used in noise reduction due to their exceptional sound-absorbing properties [4]. Many fields of industrial applications use a variety porous materials to meet the requirements of noise reduction, which nowadays are driven by regulations [2]. Research in this area has included numerous numerical and experimental studies using different types of porous materials. These materials consist of a range of organic or inorganic substances such as foams, granular materials, felts, conglomerates and other metamaterials. Several papers [13, 27] have confirmed that polymer-based synthetic fibrous material exhibit very promising sound absorption (SA) properties. All of these

materials have structures with different pore sizes (from nanometers to millimeters), are characterized by either an ordered or irregular arrangement of pores, and are obtained by different manufacturing processes/approaches. However, the macroscopic structure of the material is the basis of this classification. Based on the structure, SA materials can be cellular, fibrous, or granular [6]. Research, has focused on materials of granular structure, namely foam polypropylene panels (FPPs), which are of great interest, to the building industry.

There are several acoustic parameters that determine the categories of sound-absorbing properties of porous structures. The amount of energy accumulated by a material in proportion to the total energy incident on it, is denoted as the sound absorption coefficient (SAC). This parameter is determined, among other things, by measuring the SAC of the sample in the impedance tube or the reverberation chamber.

An exact test and computational method using two and four microphones were described for porous materials in [19]. The authors took into account the influence of sensitivity to the value of the sound absorption index, which allowed the identification of input parameters that may cause measurement uncertainty. It is worth mentioning that the value of the parameters may vary significantly depending on the model [8]. Several other factors associated with the sound absorption of porous materials, such as thickness and air gap thickness, the fiber size, density, porosity, the resistivity of air flow, etc., must also be considered. A comprehensive study of these factors has been conducted extensively in the literature [12].

Many theoretical models are available to predict the physical behavior of porous materials [7]. To improve sound absorption over a wide frequency range, both theoretical and experimental studies were carried out on materials with double porosity. A panel with perforated holes of gradually changing radius was considered in [20] and the shape of the fiber cross sectional and its impact on the acoustic properties of porous materials was analyzed in [14]. Selected theoretical models and a numerical model for materials with double porosity confirm the acoustic properties obtained during experimental tests.

The incident SAC perpendicular to a porous material can be predicted using empirical and theoretical methods. Empirical methods were developed on the basis of regression models, which rely on a large number of measurements of impedance and flow resistivity in porous materials [11, 17, 24]. Theoretical methods focus on the analysis of sound propagation in materials. The methods presented in [4, 5, 9, 18] use various parameters and physical properties to determine the impedance value and the absorption coefficient of sound. The experimental results are reflected in the numerical predictions. The prediction accuracy of the SAC has been published for several impedance prediction methods [21].

In this research, we compare the experimental results for FPP with the results of two theoretical models that have been developed over the years: the Johnson–Champoux–Allard (JCA) model [4] and the Sgard model [25]. This comparison allowed to select the proper model that shows the smallest discrepancy from the measurements. To validate the selected theoretical models, we carried out experimental studies of sound absorption on a test bench in an impedance tube. As part of the improvement of the calculation methods, a simulation of the sound absorption of a structure with a fragment of a porous expanded polypropylene panel was carried out. The results can be used to shape the frequency response to improve the SAC and efficiency of acoustic panels whose basic material is foamed polypropylene.

2. Material data

The study focused on material in the form of granules made of foamed porous polypropylene marked ARPRO 4025, ARPRO 4036 and ARPRO 5136 (further referred to as A.4025, A.4036 and A.5136). A panel made from this material is an example of a lightweight dual-purpose panel that has good sound-absorbing and insulating properties. It is characterized by properties such as abrasion resistance surface, impact resistance, fire resistance of class A, and moisture resistance. The structure of the material does not contain glass or non-fibrous materials. The manufacturer of the material in the form of granules is ARPRO, while the described dual-purpose panel is produced by the Polish company Pro EPP. Figure 1 shows samples of materials in a round shape, which corresponds to the SAC result of the tests (discs with a diameter of 34.25 mm). Table 1 provides information on the physical and acoustic properties of the materials based on samples of the same materials.

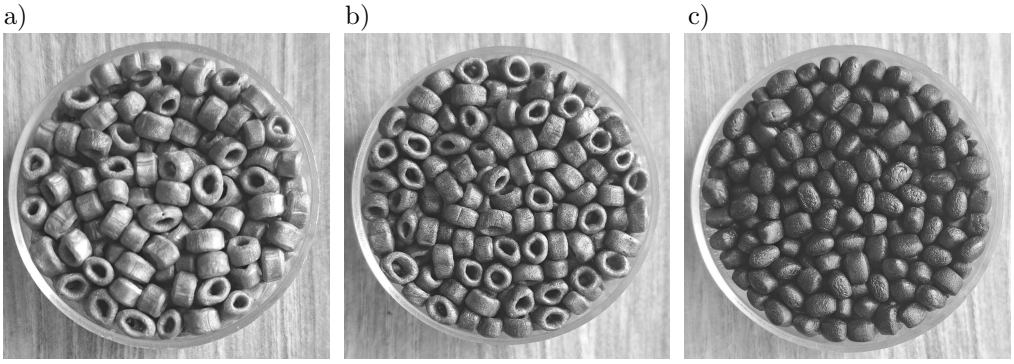

Fig. 1. Samples of expanded porous polypropylene materials:
a) ARPRO 4025, b) ARPRO 4036, c) ARPRO 5136.

Table 1. Selected parameters of the tested materials.

Material	Weight [mg]	Size [mm]	Hole size [mm]	Bulk density [g/m^3]	Thickness [mm]
A.4025	1.5	2.0–6.0	1–3.5	23.0–27.0	27
A.4036	1.5	2.0–5.0	1–3	34.0–38.0	27
A.5136	1.2	2.5–4.5	–	33.0–37.0	27

3. Poroacoustics models

As mentioned in the Introduction, over the years, several attempts have been made to develop mathematical models that adequately represent the effective frequency-dependent propagation and energy dissipation in porous materials. However, the exact values cannot be calculated in a simple way due to the complexity of the problem and the large number of influencing factors on the estimated parameters. Therefore, it is reasonable to compare the calculation results with experimental results to assess the accuracy of the model.

The subjects of the study are granules in the form of a porous panel with perforation holes, as shown in Fig. 2. The first layer of individual granules is assumed to be orientated in the same direction, perpendicular to the sound source and flow direction, and placed on a rigid back wall. Similarly, all perforated holes are directly aligned with the sound wave. The panel was assumed to consist of tightly adherent granules and perforated holes of the same shape. Each individual cell can be described as a porous material with micropores and a hole as a perforation. For materials of expanded porous polypropylene, the considered here two models are used for calculations: the Johnson–Champoux–Allard model [5] and the Sgard [25] model.

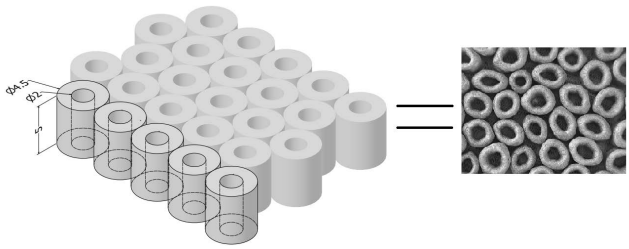

Fig. 2. Porous granule panel with perforation holes with rigid back wall.

3.1. The Johnson–Champoux–Allard model

The well-established Johnson–Champoux–Allard (JCA) model describes the viscous-inertial effects occurring and dissipating inside porous media. It is commonly used to model the propagation of sound in porous, air-filled media. The

JCA model takes into account physical non-acoustic parameters such as porosity ϕ, static flow resistivity σ, tortuosity α_∞, and the viscous and thermal characteristic lengths Λ, Λ' [5].

According to Johnson, Koplik, and Dashen the effective density of air in porous materials is given by [14, 16]:

$$\rho_e = \alpha_\infty \rho_0 \left[1 + \frac{\sigma\phi}{i\omega\alpha_\infty\rho_0}\left(1 + i\frac{4\omega\alpha_\infty^2\rho_0\eta}{\sigma^2\Lambda^2\phi^2}\right)^{1/2}\right], \tag{3.1}$$

where ρ_0 is the air density in free space, ω is the angular frequency, associated with the frequency f, according to the relation $\omega = 2\pi f$, α_∞ is responsible for the value of the upper limit of the tortuosity, η is the viscosity of the air, σ denotes the static air resistance, ϕ expresses the value of porosity, Λ is the viscous characteristic length. On the other hand, according to Champoux and Allard, the dynamic bulk modulus of air in porous materials is given by [10, 14]:

$$K_e = \frac{\gamma P_0}{\gamma - (\gamma-1)\left[1 + \frac{8\eta}{i\omega\rho_0 B^2\Lambda'^2}\left(1 + i\frac{\omega\rho_0 B^2\Lambda'^2}{16\eta}\right)^{1/2}\right]^{-1}}, \tag{3.2}$$

where P_0 is the atmospheric pressure, γ is the coefficient of specific heat of the air, and B^2 is the Prandtl number.

The panel is assumed to be an isotropic porous material, and the normal sound absorption coefficient α_0 of the panel was determined as [4]:

$$\alpha_0 = 1 - \left|\frac{Z_s - \rho_0 c_0}{Z_s + \rho_0 c_0}\right|^2, \tag{3.3}$$

where Z_s determines the surface impedance for porous materials located on a rigid wall and is expressed as [26]:

$$Z_s = -Z_c \cot(kd). \tag{3.4}$$

In the above expression Z_c denotes the characteristic impedance, k is the complex wavenumber, and d is the thickness of the material. The impedance Z_c and the wavenumber k can be determined from the effective density ρ_e and the bulk modulus K_e as follows:

$$Z_c = \frac{\sqrt{\rho_e K_e}}{\phi} \qquad \text{and} \qquad k = \omega\sqrt{\frac{\rho_e}{K_e}}. \tag{3.5}$$

The coefficient values for the JCA model used in the calculations are summarized in Table 2.

Measurements of the absorption coefficient performed and discussed in Sec. 4 were used to evaluate the accuracy of the JCA model.

TABLE 2. Acoustic parameters of porous materials for the JCA model.

Material	σ [kPa · s · m^{-2}]	α_∞	ϕ	Λ [m]	Λ' [m]
A.4025	20	1.22	0.43	5.00E−05	1.00E−04
A.4036	25	1.22	0.53	5.00E−05	1.00E−04
A.5136	30	1.36	0.68	5.00E−05	1.00E−04

3.2. The Sgard model

The Sgard model focuses on materials known as mesoperforated materials, commonly referred to as double porosity materials. This analytical model assumes that the medium is periodic and stationary in space, and there is a difference between the size of micro and meso perforations. Acoustic performance is governed by the size of the perforation, porosity and the aspect ratio, which depends on the shape of the perforation and the arrangement of the pores [25].

The Sgard model, similarly to the JCA model, contains some input parameters describing the material, including: porosity ϕ_m, static flow resistivity σ_m, tortuosity α_{∞_m}, viscous and thermal characteristic lengths Λ_m, Λ'_m, thermal permeability $\Theta_m(0)$, the radius of the hole R, and meso-porosity ϕ_p.

Similarly, a material with the described parameters of given values was considered. The parameters with the index m characterize the properties of the material with micro-perforations, while the parameter with the index p corresponds to meso-perforations. The values of the individual parameters were determined based on available data and collected in Table 3.

TABLE 3. Acoustic parameters of porous materials for the Sgard model.

Material	σ [kPa · s · m^{-2}]	α_∞	ϕ	Λ [m]	Λ' [m]	Θ_m	ϕ_p	R
A.4025	20	1.22	0.43	5.0E−05	1.0E−04	1	0.99	2.0E−03
A.4036	25	1.22	0.53	5.0E−05	1.0E−04	1	0.99	1.7E−03
A.5136	30	1.36	0.68	5.0E−05	1.0E−04	1	0.99	1.2E−03

The characteristic impedance and propagation constant in a dual-porosity medium during sound propagation parallel to the pores were determined using the following expressions [25]:

$$Z_c = \sqrt{\rho_{dp} K_{dp}} \qquad \text{and} \qquad k = \omega \sqrt{\frac{\rho_{dp}}{K_{dp}}}. \tag{3.6}$$

The generalized Darcy's law, analogous to single-porosity media, accounts for dynamic permeability Π_{dp} and bulk modulus K_{dp} depending on the meso-

geometry. The effective density ρ_{dp} is related to dynamic permeability by the following relationship:

$$\rho_{dp} = \frac{\eta_f}{j\omega\Pi_{dp}}, \tag{3.7}$$

where η_f represents the dynamic viscosity of the fluid. If a single cell consists of a cylindrical shape of a radius R, the dynamic permeability of the material in the perpendicular direction is given by [22, 23] as:

$$\Pi_{dp} = (1-\phi_p)\,\Pi_m - \Pi_p, \tag{3.8}$$

where Π_p represents the dynamic permeability of a single-porosity medium with a microporous structure and Π_m represents the dynamic permeability in the direction normal to the medium consisting of a network of pores, where the microporous part has been replaced by an impermeable material. The value of Π_m can be calculated using, for example, the Johnson model [16].

Authors [22, 23] also proposed the dynamic bulk modulus K_{dp} for a double-porosity material as:

$$K_{dp} = \left[\frac{1}{K_p} + (1-\phi_p)\,\frac{F_d\left(\omega\frac{P_0}{\phi_m K_m}\right)}{K_m}\right]^{-1}, \tag{3.9}$$

where K_p and K_m are, respectively, the dynamic bulk moduli of a single-porosity medium and a medium consisting of a network of pores, where the microporous part has been replaced by an impermeable material. The parameter P_0 denotes the static ambient pressure, while F_d is a frequency-dependent function that represents the ratio of the pressure in the micropores to the pressure in the pores of the material. In this context, the surface impedance Z_{dp} of the material with thickness e and backed by the material with surface impedance Z_s is given by [25]:

$$Z_{dp} = Z_c\frac{Z_c - jZ_s\cot ke}{Z_s - jZ_c\cot ke}. \tag{3.10}$$

The Sgard model is described in detail in [25] with a specification of equations and relationships. On their basis, the absorption coefficient of sound incident perpendicular to the surface is given by [25]:

$$\alpha = \frac{4\mathrm{Re}\left[z_{dp}\right]}{\left(\mathrm{Re}\left[z_{dp}\right]+1\right)^2 + \mathrm{Im}\left[z_{dp}\right]^2}, \tag{3.11}$$

where z_{dp} is given by:

$$z_{dp} = \frac{Z_{dp}}{\rho_a c_\alpha}. \tag{3.12}$$

The parameters ρ_α and c_α are the density and sound speed in the medium through which the incident wave propagates. The symbols Re and Im denote the real and imaginary parts of the Z_{dp} component, respectively.

4. Experimental research on the sound absorption coefficient of normal incidence

The experimental research was carried out in the Laboratory of Modelling Acoustic Phenomena of the University of Rzeszów. The SAC was determined using a Siemens impedance tube, type Mecanum Inc. S/N: 2444-408. A schematic diagram of the impedance tube used is shown in Fig. 3. The system performs measurements according to a specific standard: PN-EN ISO 10534-2:2003 and ASTM E-1050, ASTM E-2611 (TL) [1, 3, 15]. The test stand and measuring device were the same as in the tests described in [19]. The laboratory bench specification was based on a Siemens impedance tube, type Mecanum Inc., a Siemens LMS SCADAS Mobile analyzer, a computer with Simcenter Testlab software, and PCB measurement microphones type 378A14 1/4″, spaced at 65 or 29 mm intervals for low and high frequencies, respectively. The microphones were calibrated and the calibration parameters were set to 114 dB at 1000 Hz. The SAC has been determined on the basis of averaged results in the frequency range of 50 to 5700 Hz. Measurements were made for the atmospheric conditions that prevailed in the laboratory, that is, at a temperature of 20°C and an atmospheric pressure of 1000 hPa.

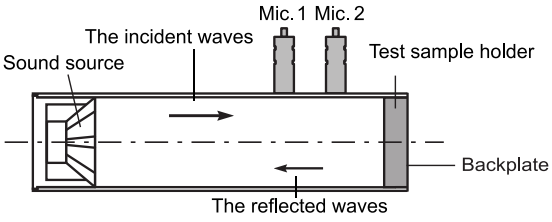

Fig. 3. Schematic diagram of an impedance tube used for measuring the sound attenuation coefficient.

The experimental procedure involved testing three types of granules of different bulk density, grain fractions, and shapes, all made of expanded polypropylene. As intended, the samples were prepared for measurement in such a way that the first layer of individual granules was oriented in the same direction, perpendicular to both the sound source and flow direction. The subsequent layers were randomly filled with granules in such a way as to ensure free friction between successive particles. The measurement samples, with a cylinder shape with a diameter of 34.25 mm and a length of 27 mm, were assumed.

5. Analysis and comparison of results

Experimental studies of sound absorption were carried out to validate the proposed theoretical models: the JCA model and the Sgard model (the double porosity materials). The sound absorption performance was determined for materials with double porosity in the form of granules with perforated holes. The single cell under consideration, shown in Fig. 2 has a thickness of 27 mm, a diameter of 34.25 mm, and a perforated hole profile of 1–3 mm depending on the material. Physical parameters and characteristic acoustic parameters such as porosity ϕ, static flow resistivity σ, tortuosity α_∞, and the viscous and thermal characteristic lengths Λ and Λ' are collected in Tables 1 and 2. A comparison of the SAC for the described theoretical models and experimental measurements of the granules is shown in Figs. 4, 5, and 6.

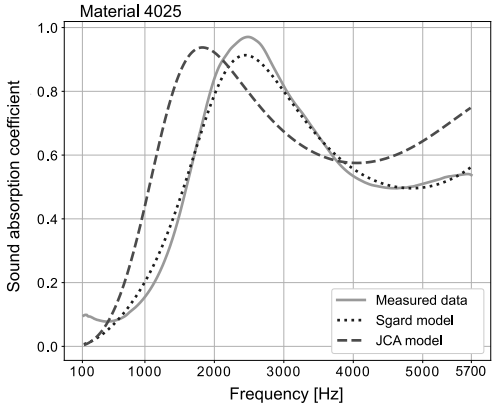

Fig. 4. SAC: comparison of the JCA model, the Sgard model, and measurement for the 4025 material.

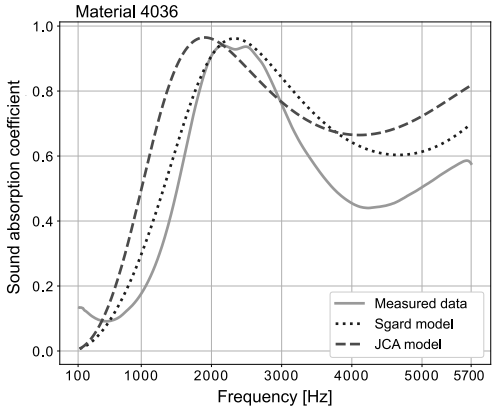

Fig. 5. SAC: comparison of the JCA model, the Sgard model, and measurement for the 4036 material.

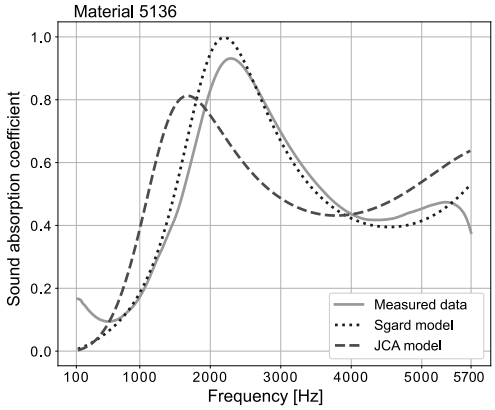

Fig. 6. SAC: comparison of the JCA model, the Sgard model, and measurement for the 5136 material.

It can be seen that the best agreement between the theoretical methods and the measurements of the porous materials considered was obtained for the Sgard model. The selected model quite effectively reproduced the absorption coefficient of both Type 4025 and Type 5136 samples across the full frequency range (Figs. 4 and 6). The certain small discrepancy that can be observed between the Sgard model and the measurement results in Fig. 6 can be explained by the arrangement of the sample. The first layer of the sample tested was placed strictly perpendicular to the sound sources, while each subsequent layer was randomized, which could affect the results.

In the case of the sample Type 4036, the Sgard model retained the characteristic transitions and resonant frequencies, however, at higher frequencies, i.e., above 2500 Hz, it exhibited a bit higher values of SAC than those observed in the measurements. On the other hand, the JCA model showed even higher SAC values, with an extremum of SAC = 0.95, calculated theoretically, occurring at $f = 1800$ Hz, which is clearly below the values obtained from the measurements.

6. Summary and conclusions

Several papers have confirmed that polymer-based porous structures exhibit very promising SACs; however, the acoustic behavior of these materials is influenced by several parameters such as the size of the perforation, the porosity of the material, and the shape of the individual piece, all of which directly affect the performance of the SAC. Currently, there remains a need for methods to design/determine SAC values depending on the various applications of the sound-absorbing structures.

The purpose of the research was to compare theoretical methods for determining the SAC with experimental results for panels made from expanded porous polypropylene materials, namely: ARPRO 4025, ARPRO 4036, and ARPRO 5136.

It can be seen from the obtained results that the frequency characteristics of the materials considered based on expanded porous polypropylene can be efficiently designed with the Sgard theoretical model. This model demonstrated strong consistency with the characteristics obtained from measurements. The small difference between the Sgard model, predictions, and the measurement characteristics, as shown in the figures, may result from several factors. These include difficulties in estimating some of the parameters and physical properties required to determine the absorption coefficient in the Sgard model and the arrangement of granules in the layers of test samples. The findings can be used to improve the SAC of acoustic panels made from foamed polypropylene.

References

1. PN-EN ISO 10534-2:2003, *Acoustics-Determination of Sound Absorption Coefficient and impedance in Impedance Tubes – Part 2: Transfer-Function Method.*
2. PN-B-02151-2:2018-01, *Building Acoustics-Protection against Noise in Buildings. Part 2: Requirements for Permissible Sound Levels in Rooms.*
3. ASTM E1050, *Standard Test Method for Impedance and Absorption of Acoustical Materials Using a Tube, Two Microphones and a Digital Frequency Analysis System*, 2019.
4. Allard J.-F, Atalla N., *Propagation of Sound in Porous Media: Modelling Sound Absorbing Materials*, John Wiley & Sons, 2009, https://doi.org/10.1002/9780470747339.
5. Allard J.F., Champoux Y., New empirical equations for sound propagation in rigid frame fibrous materials, *The Journal of the Acoustical Society of America*, **91**(6): 3346–3353, 1992, https://doi.org/10.1121/1.402824.
6. Arenas J.P., Crocker M.J., Recent trends in porous sound absorbing materials, *Sound & Vibration*, **44**(7): 12–17, 2010.
7. Atalla N., Introduction to the numerical modeling and experimental characterization of porous materials, *Public Technical Course*, Graz, Austria, pages 1–2, 2014.
8. Batko W., Pawlik P., Wszołek G., Sensitivity analysis of the estimation of the single-number sound absorption evaluation index DL_α, *Archives of Acoustics*, **42**(4): 689–696, 2017, https://doi.org/10.1515/aoa-2017-0071.
9. Cai Z., Li X., Gai X., Zhang B., Xing T., An empirical model to predict sound absorption ability of woven fabrics, *Applied Acoustics*, **170**: 107483, 2020, https://doi.org/10.1016/j.apacoust.2020.107483.
10. Champoux Y., Allard J.-F., Dynamic tortuosity and bulk modulus in air-saturated porous media, *Journal of Applied Physics*, **70**(4): 1975–1979, 1991, https://doi.org/10.1063/1.349482.

11. Delany M.E., Bazley E.N., Acoustical properties of fibrous absorbent materials, *Applied Acoustics*, **3**(2): 105–116, 1970, https://doi.org/10.1016/0003-682X(70)90031-9.

12. Dev B., Rahman M.A., Repon M.R., Rahman M.M., Haji A., Nawab Y., Recent progress in thermal and acoustic properties of natural fiber reinforced polymer composites: preparation, characterization, and data analysis, *Polymer Composites*, **44**(11): 7235–7297, 2023, https://doi.org/10.1002/pc.27633.

13. Egab L., Wang X., Fard M., Acoustical characterisation of porous sound absorbing materials: a review, *International Journal of Vehicle Noise and Vibration*, **10**(1–2): 129–149, 2014, https://doi.org/10.1504/IJVNV.2014.059634.

14. Hirosawa K., Numerical study on the influence of fiber cross-sectional shapes on the sound absorption efficiency of fibrous porous materials, *Applied Acoustics*, **164**: 107222, 2020, https://doi.org/10.1016/j.apacoust.2020.107222.

15. ASTM International, ASTM E2611-09, *Standard Test Method for Measurement of Normal Incidence Sound Transmission of Acoustical Materials Based on the Transfer Matrix Method*, ASTM, 2009.

16. Johnson D.L., Koplik J., Dashen R., Theory of dynamic permeability and tortuosity in fluid- saturated porous media, *Journal of Fluid Mechanics*, **176**: 379–402, 1987, https://doi.org/10.1017/S0022112087000727.

17. Kino N., Further investigations of empirical improvements to the Johnson–Champoux–Allard model, *Applied Acoustics*, **96**: 153–170, 2015, https://doi.org/10.1016/j.apacoust.2015.03.024.

18. Kino N., Ueno T., Improvements to the Johnson–Allard Model for rigid-framed fibrous materials, *Applied Acoustics*, **68**(11–12): 1468–1484, 2007, https://doi.org/10.1016/j.apacoust.2006.07.005.

19. Kunio J., Yoo T., Jou K., Bolton J.S., Enok J., A comparison of two and four microphone standing wave tube procedures for estimating the normal incidence absorption coefficient, [in:] *38th International Congress and Exposition on Noise Control Engineering 2009 (INTER-NOISE 2009), Ottawa, Canada*, Stuart Bolton J., Burroughs C., Gover B. [Eds.], pp. 1057–1065, Curran Associates, Inc., Red Hook, NY, 2010.

20. Liu X., Ma X., Yu C., Xin F., Sound absorption of porous materials perforated with holes having gradually varying radii, *Aerospace Science and Technology*, **120**: 107229, 2022, https://doi.org/10.1016/j.ast.2021.107229.

21. Oliva D., Hongisto V., Sound absorption of porous materials – Accuracy of prediction methods, *Applied Acoustics*, **74**(12): 1473–1479, 2013, https://doi.org/10.1016/j.apacoust.2013.06.004.

22. Olny X., *Acoustic Absorption of Porous Media with Single and Double Porosity-Modeling and Experimental Solution* [in French], PhD thesis, ENTPE-Institut National des Sciences Appliquées de Lyon, 281 p. 1999.

23. Olny X., Boutin C., Acoustic wave propagation in double porosity media, *The Journal of the Acoustical Society of America*, **114**(1): 73–89, 2003, https://doi.org/10.1121/1.1534607.

24. Wu Q., Empirical relations between acoustical properties and flow resistivity of porous plastic open-cell foam, *Applied Acoustics*, **25**(3): 141–148, 1988, https://doi.org/10.1016/0003682X(88)90090-4.

25. Sgard F.C., Olny X., Atalla N., Castel F., On the use of perforations to improve the sound absorption of porous materials, *Applied Acoustics*, **66**(6): 625–651, 2005, https://doi.org/10.1016/j.apacoust.2004.09.008.

26. Whitley R.J., Hromadka II T.V., Theoretical developments in the complex variable boundary element method, *Engineering Analysis with Boundary Elements*, **30**(12): 1020–1024, 2006, https://doi.org/10.1016/j.enganabound.2006.08.002.

27. Świrk P., Leniowska L., Korzyńska K., Acoustic properties of biodegradable materials in the low and medium frequency range, *Vibrations in Physical Systems*, **35**(2): 2024209, 2024, https://doi.org/10.21008/j.0860-6897.2024.2.08.

Received August 21, 2024; accepted version December 9, 2024.
Online first January 28, 2025.